Heliospheric Remote-Sensing Observations and Modelling: An Outlook to a Long-Standing View from L5.

Mario M. Bisi *(Mario.Bisi@stfc.ac.uk)* ***(1), Bernard V. Jackson (2), Dusan Odstrcil (3,4), David F. Webb (5), Chin-Chun Wu (6), Munetoshi Tokumaru (7), J. Americo Gonzalez-Esparza (8), Richard A. Fallows (9), Elizabeth A. Jensen (10), P. Paul Hick (2), Andrew Buffington (2), and Hsiu-Shan Yu (2).***

(1) Science and Technology Facilities Council – Rutherford Appleton Laboratory, England, UK
(2) University of California, San Diego, CA, USA
(3) George Mason University, VA, USA
(4) NASA GSFC, MD, USA
(5) Boston College, MA, USA
(6) Naval Research Laboratory, DC, USA
(7) Nagoya University, Japan
(8) UNAM, Mexico
(9) ASTRON, The Netherlands
(10) Planetary Sciences Institute, AZ, USA.

Science & Technology Facilities Council

RAL Space

Today's Heliospheric-Imaging Talks

- This talk – concentrates on large-scale three-dimensional (3-D) modelling (including MHD) and complementary techniques.
- Harrison and Davies talk – provides the context of L5 having been there already with the STEREO-B HIs and the bigger picture of visible-light heliospheric imaging and what we have learned from it thus far with an emphasis on the STEREO HIs.
- Howard and DeForest talk – provides discussion over visible-light heliospheric design considerations, lessons learned thus far from visible-light heliospheric imaging, and looking forward to the next generation of visible-light heliospheric imagers.
- Tappin talk – describes a possible next step in advancing the science of visible-light heliospheric imaging by looking at the possibilities of a polarised heliospheric imaging.

Outline

- Brief Introduction to the Multi-Site Interplanetary Scintillation (IPS) Experiment (Radio Heliospheric Imaging)
- UCSD 3-D Computer Assisted Tomography
- Complementarities of Radio and Visible-Light Heliospheric Imaging and MHD Modelling
- 3-D Tomography with Visible-Light Data
- Progress Towards Heliospheric Faraday Rotation (FR) Determination and Verification, Including 3-D Tomography and input to ENLIL MHD Modelling
- Next Steps for 3-D Tomography and MHD with Visible-Light Data
- Brief Summary and Outlook to a Long-Standing View from L5

Brief Introduction to the Multi-Site Interplanetary Scintillation (IPS) Experiment (Radio Heliospheric Imaging)

Multi-Site IPS (1)

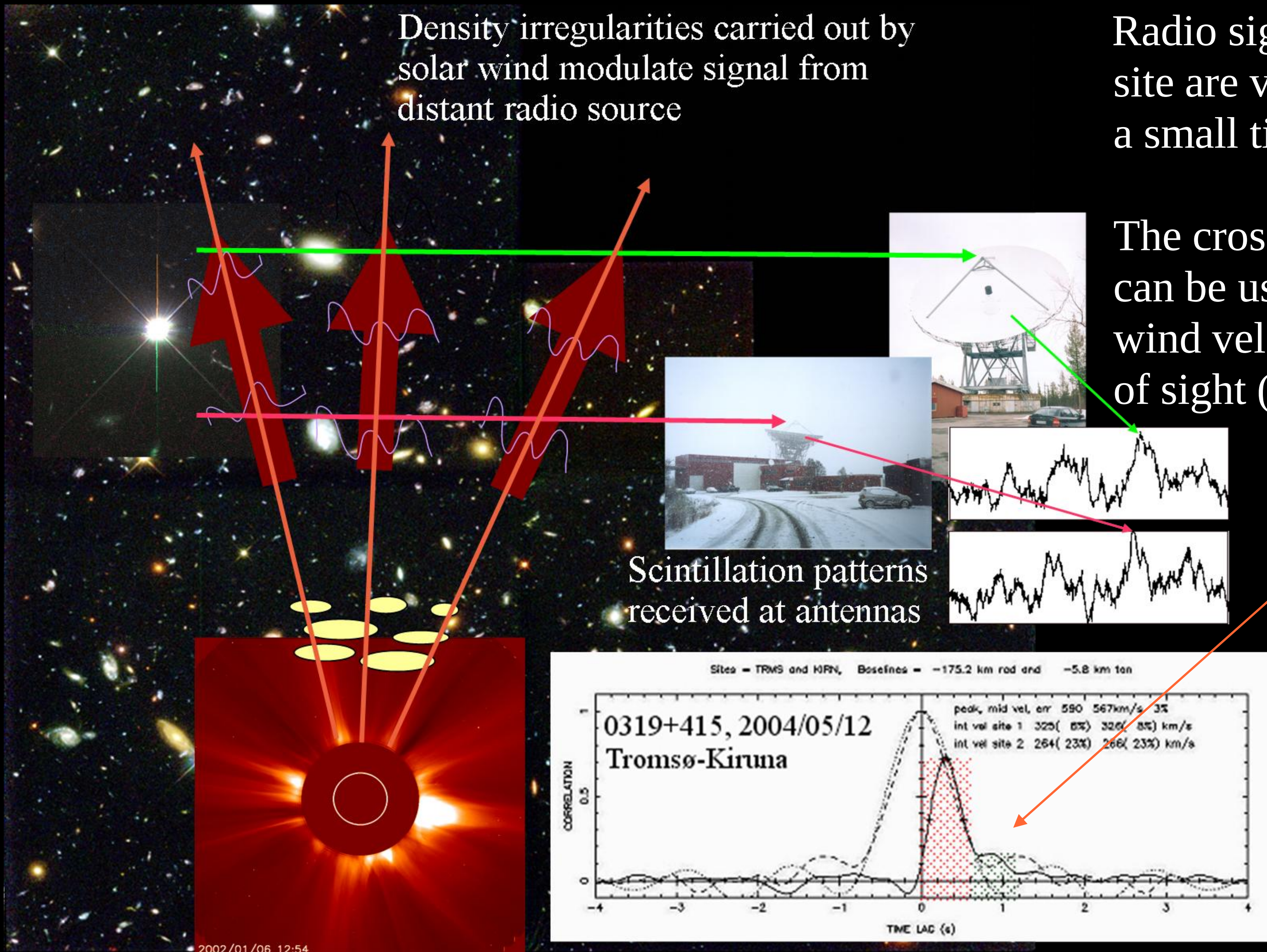

Hubble Deep Field – HST (WFPC2) 15/01/96 – Courtesy of R. Williams and the HDF Team and NASA

Radio signals received at each site are very similar except for a small time-lag.

The cross-correlation function can be used to infer the solar wind velocity(s) across the line of sight (LOS).

(Not to scale)

IPS is most-sensitive at and around the P-Point of the LOS to the Sun and is only sensitive to the component of flow that is perpendicular to the LOS; it is variation in intensity of astronomical radio sources on timescales of ~0.1s to ~10s that is observed.

Multi-Site IPS (2)

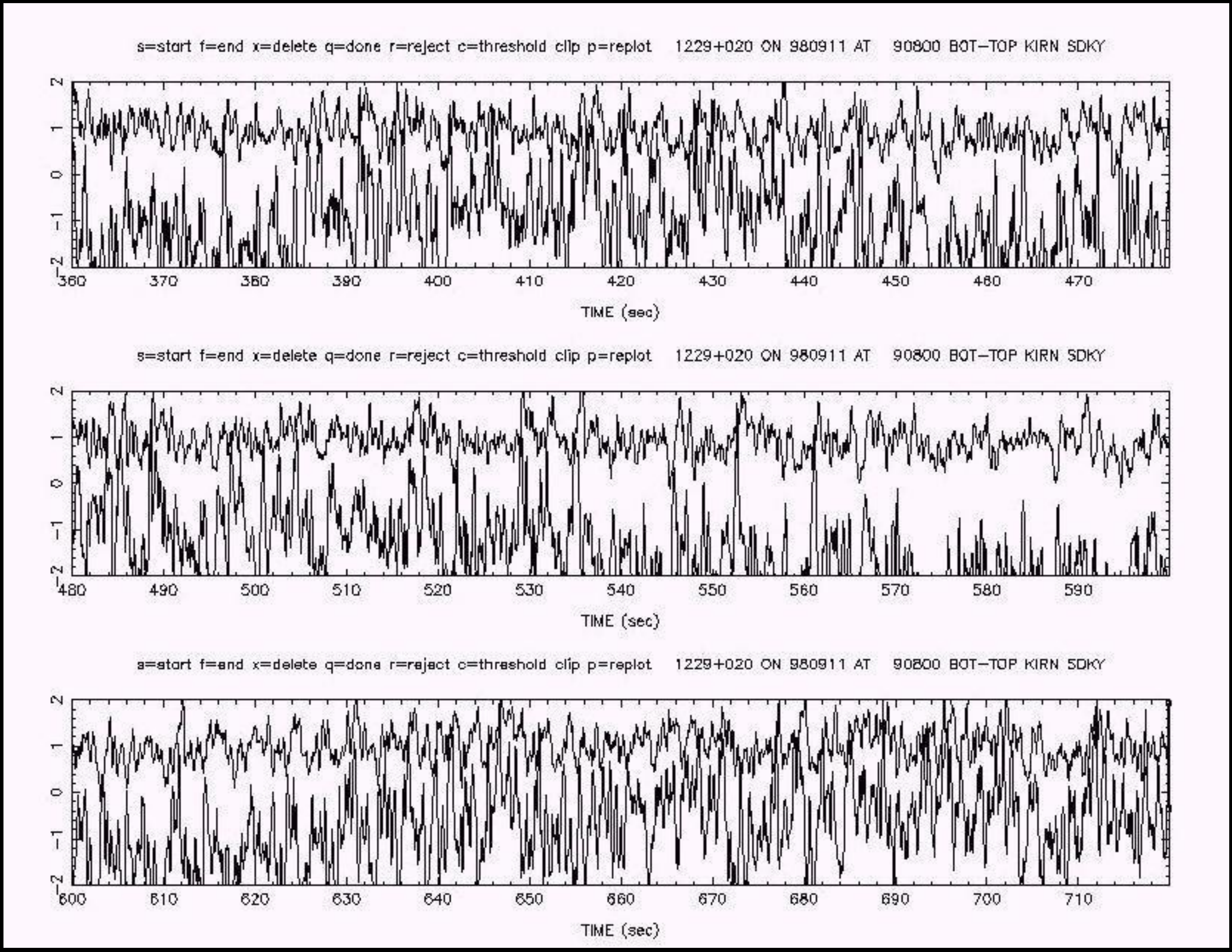

IPS (*g*-level/density)

Density Turbulence

- Scintillation index, m, is a measure of level of turbulence
- Normalized Scintillation index, g = m(R) / <m(R)>

- **g > 1 → enhancement in δNe**
- **g ≈ 1 → ambient level of δNe**
- **g < 1 → rarefaction in δNe**

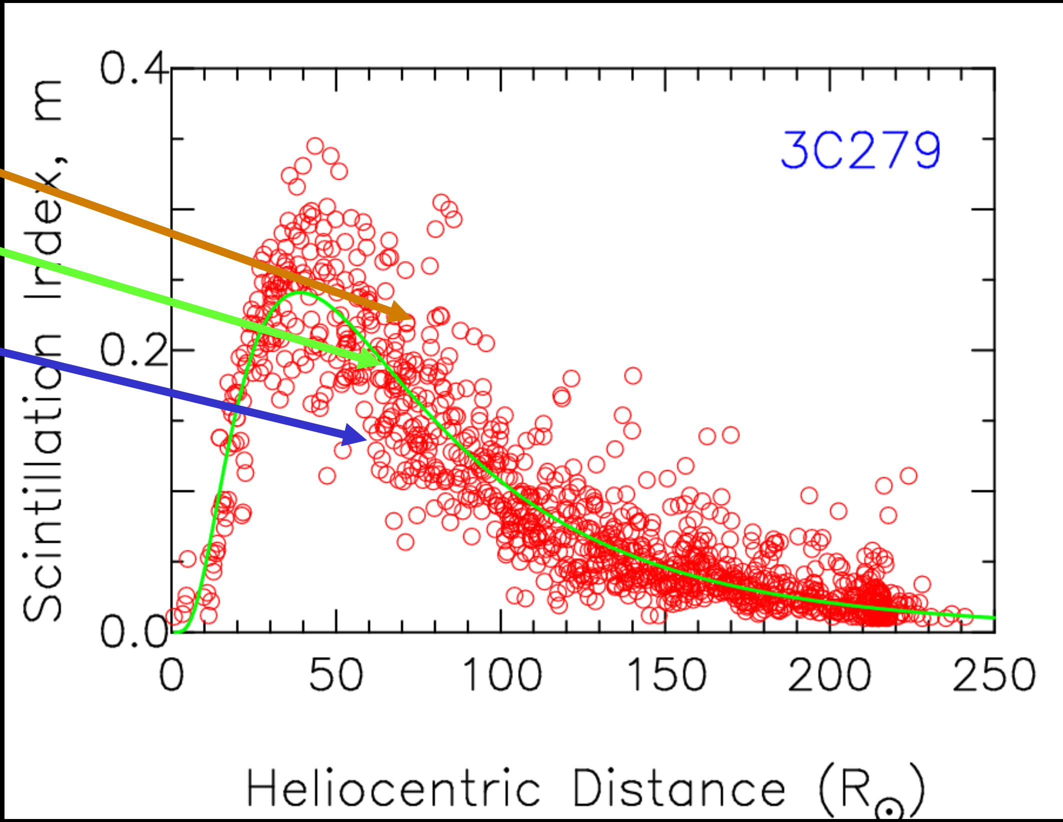

(Courtesy of Periasamy K. Manoharan)

Scintillation enhancement with respect to the ambient wind identifies the presence of a region of increased turbulence/density and possible CME along the line-of-sight to the radio source

UCSD 3-D Computer Assisted Tomography

UCSD 3-D Tomography Simple View

Heliospheric C.A.T. Analyses: example line-of-sight distribution for each sky location to form the source surface of the 3D reconstruction.

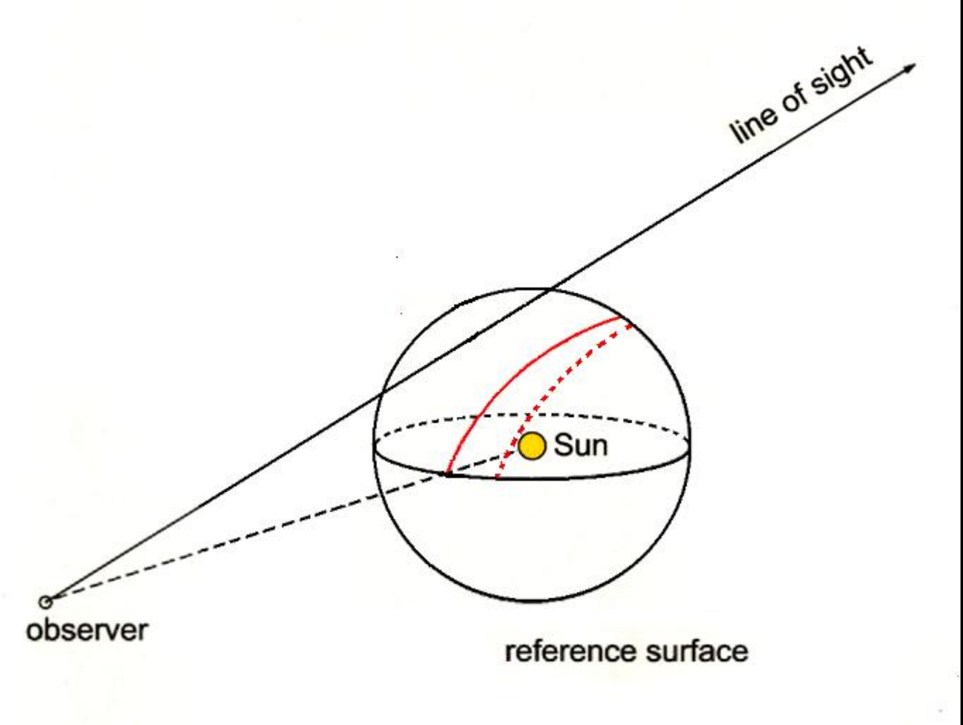

STELab IPS

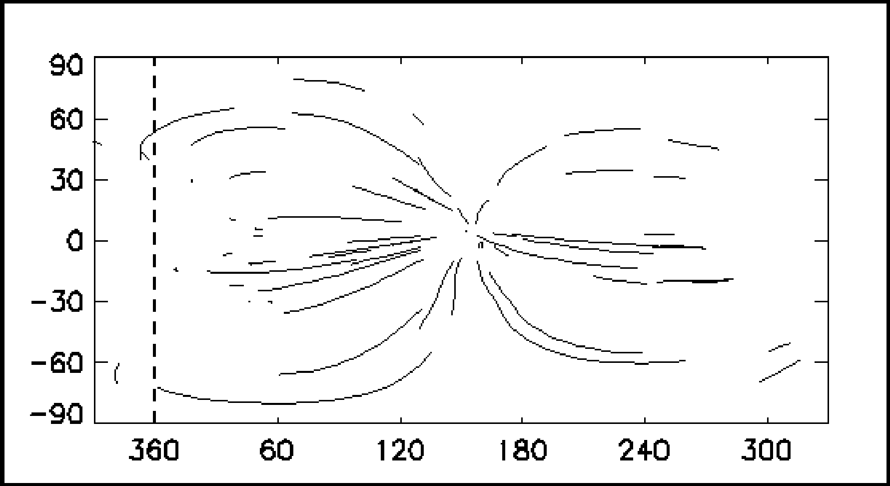

13 July 2000

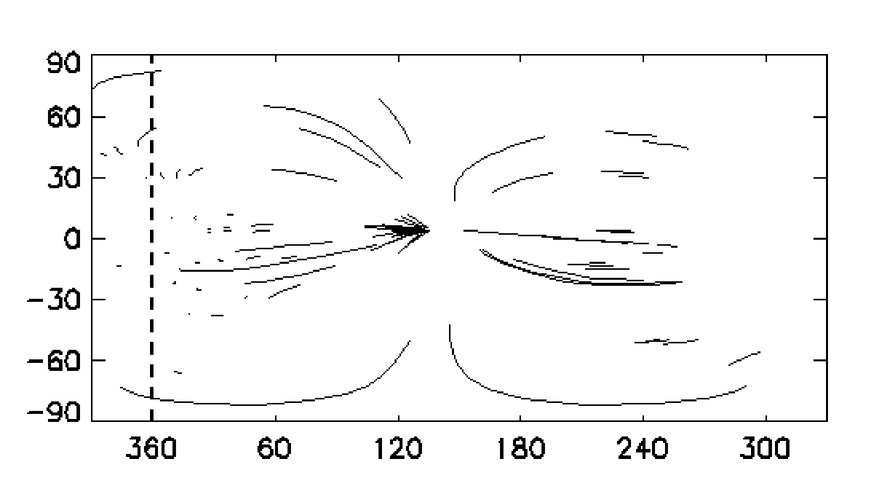

14 July 2000

UCSD 3-D Tomography for Forecasting

UCSD

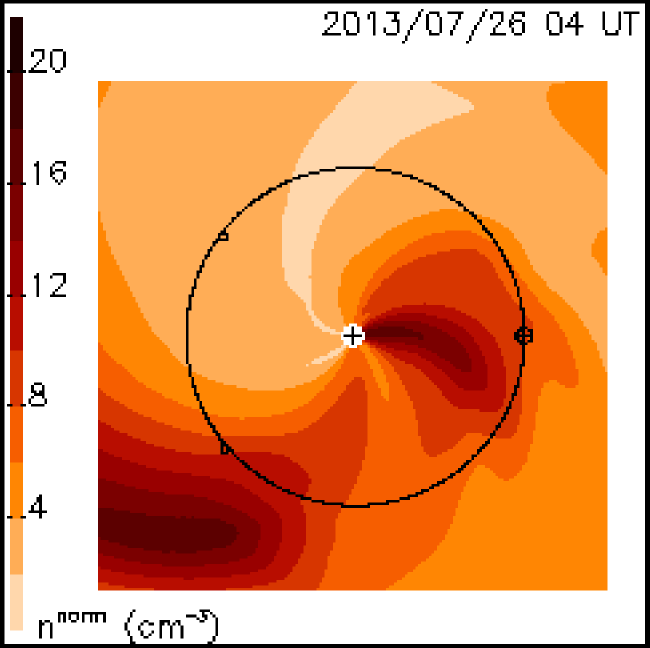

KSWC

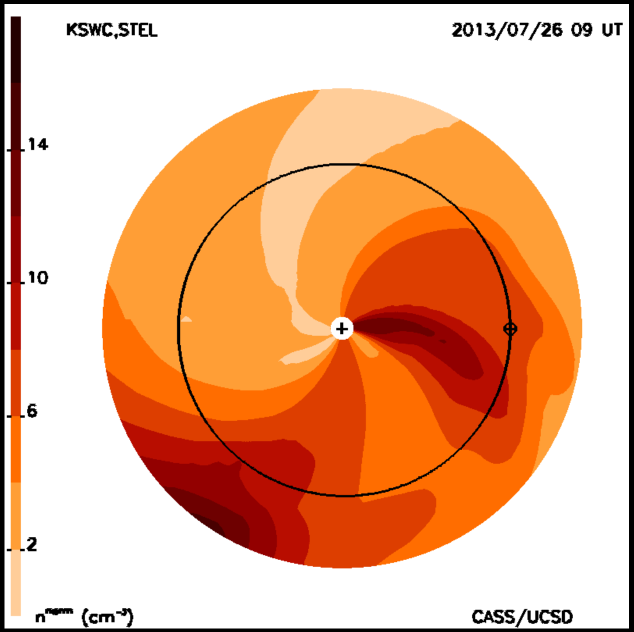

http://ips.ucsd.edu/

http://www.spaceweather.go.kr/models/ips

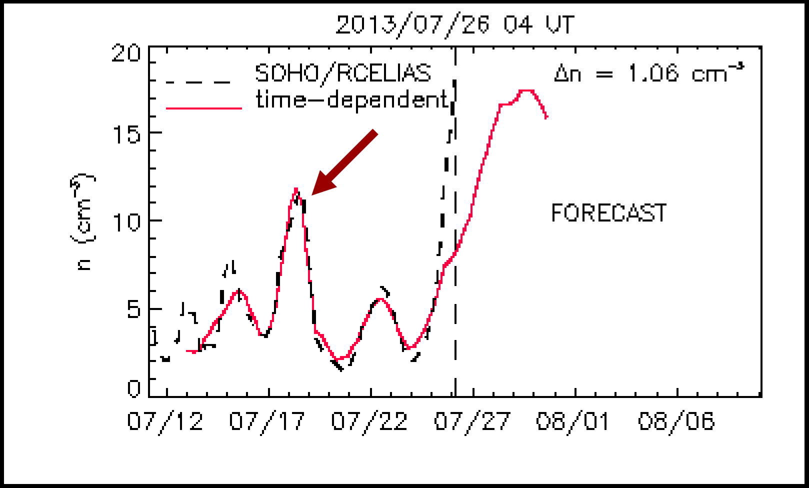

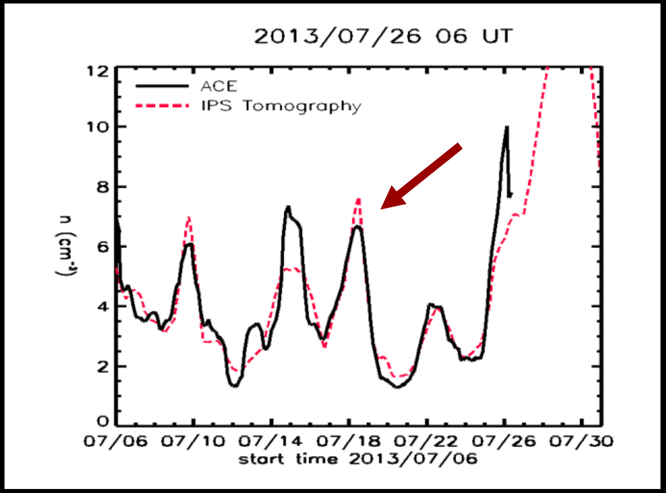

Complementarities of Radio and Visible-Light Heliospheric Imaging and MHD Modelling

IPS with LOFAR: The First CME Detection

- R.A. Fallows, A. Asgekar, M.M. Bisi, A.R. Breen, S. ter-Veen, and on behalf of the LOFAR Collaboration, “The Dynamic Spectrum of Interplanetary Scintillation: First Solar Wind Observations on LOFAR”, Solar Physics “Observations and Modelling of the Inner Heliosphere” Topical Issue (Guest Editors M.M. Bisi, R.A. Harrison, and N. Lugaz), 285 (1-2), 127-139, 2013.

Taken from - Bisi, M.M., S.A. Hardwick, R.A. Fallows, J.A. Davies, R.A. Harrison, E.A. Jensen, H. Morgan, C.-C. Wu, A. Asgekar, M. Xiong, E. Carley, G. Mann, P.T. Gallagher, A. Kerdraon, A.A. Konovalenko, A. MacKinnon, J. Magdalenić, H.O. Rucker, B. Thide, C. Vocks, *et al*., “The First Coronal Mass Ejection Observed with the LOw Frequency ARray (LOFAR)”, submitted to The Astrophysical Journal Supplementary Series, (and references therein), 2014/2015.

STEREO COR2-B CME Observations

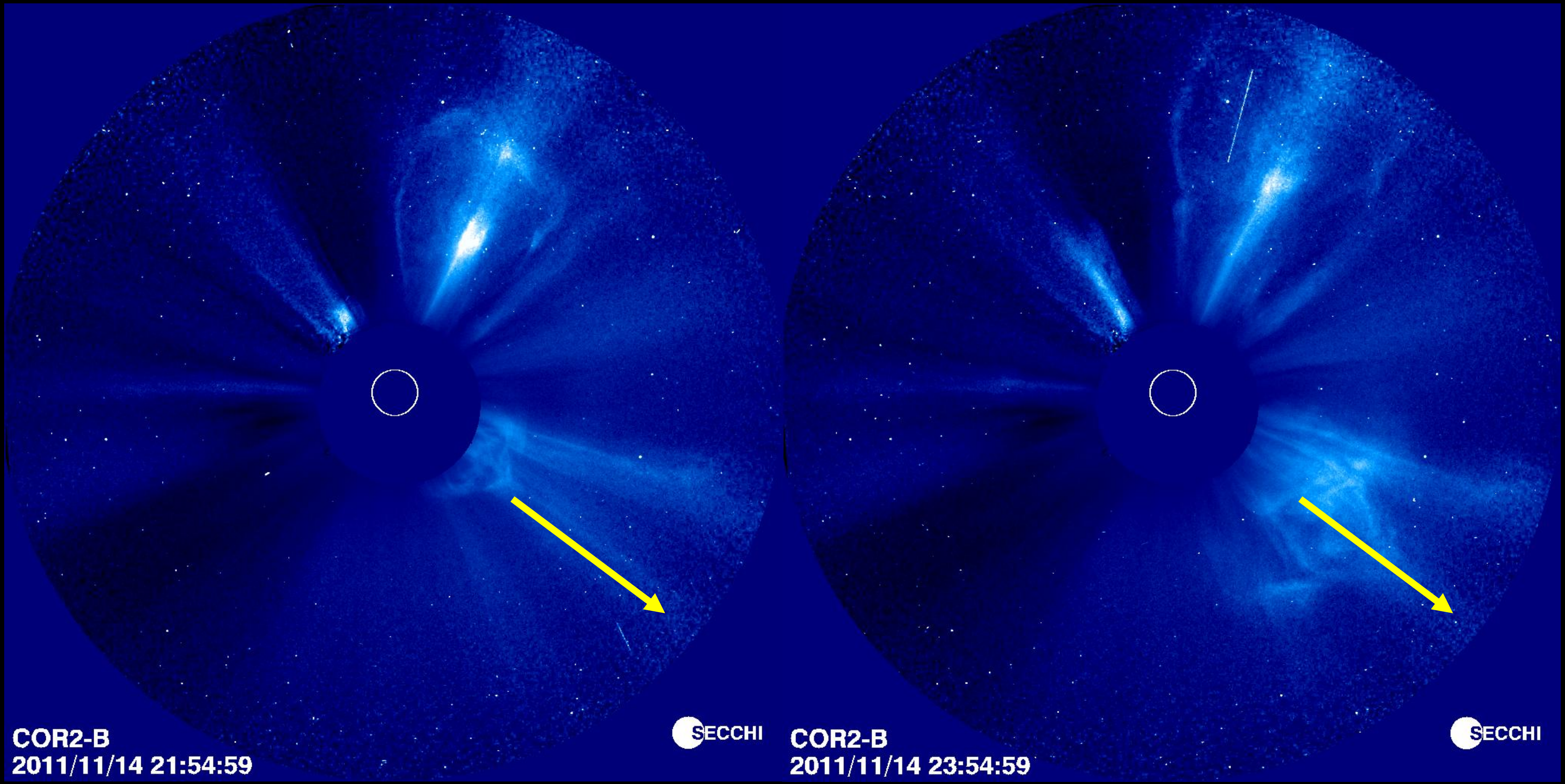

- STEREO COR2 imagery of the CME seen to be going to the South-West from this viewpoint, *i.e*. South and Mars/Earth-ward (to the right of each image). Left: COR2-B on 14/11/11 at 21:54:59UT and Right: COR2-B on 14/11/11 at 23:54:59UT.

STEREO-A HI Observations of the CME

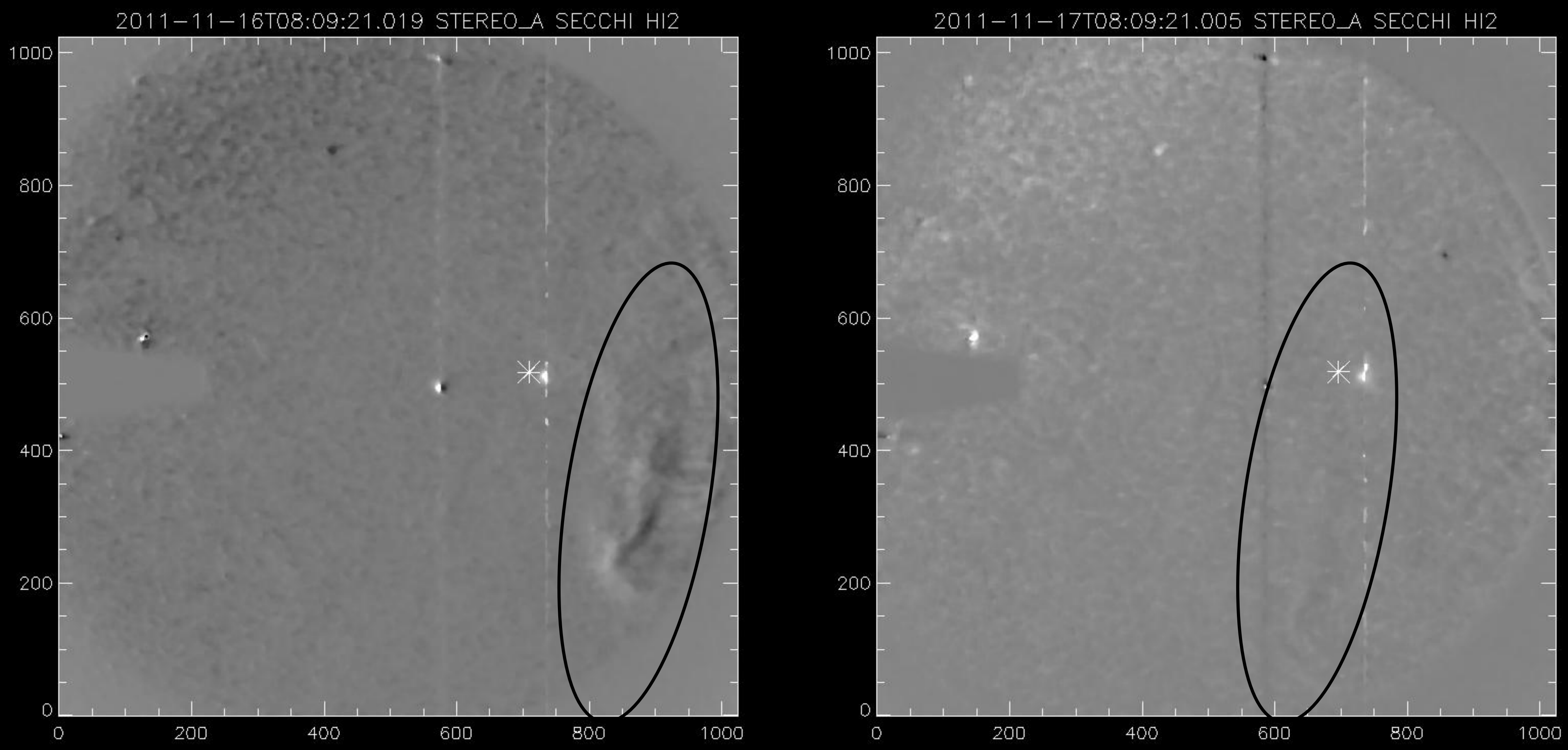

- STEREO-A HI imagery shows the Northern-most flank of the CME (inside the ellipse) crossing over the line of sight (*) to the radio source at the same time as the LOFAR observation of IPS.

The First CME with LOFAR…

- Observations of J1256-057 (3C279) detecting a CME with LOFAR on 17 November 2011 and (briefly) its comparison so far with other remote-sensing observations and modelling.

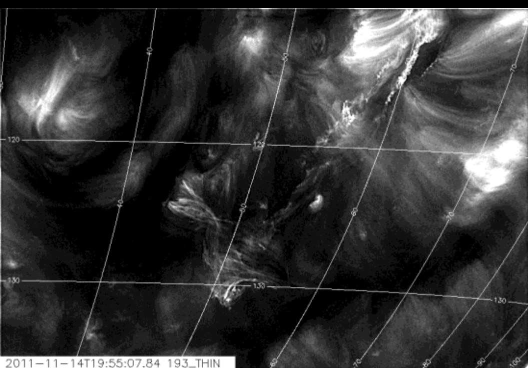

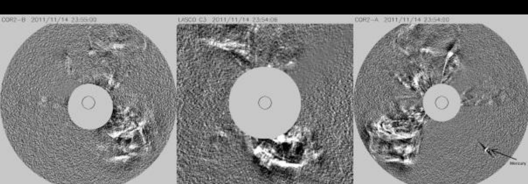

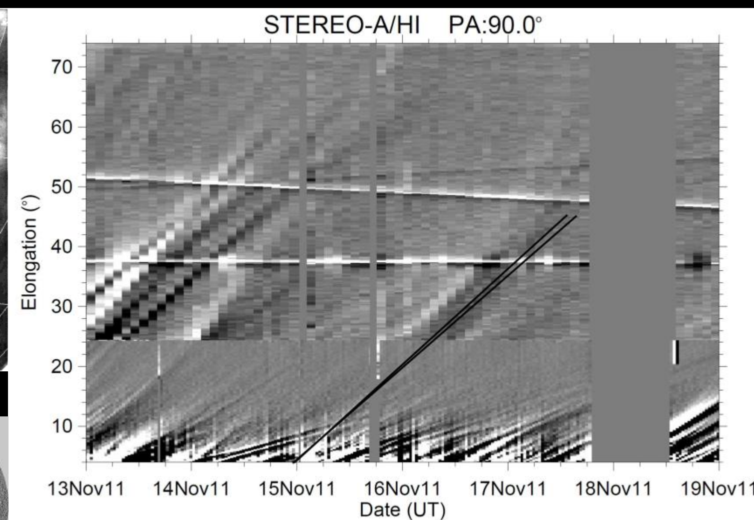

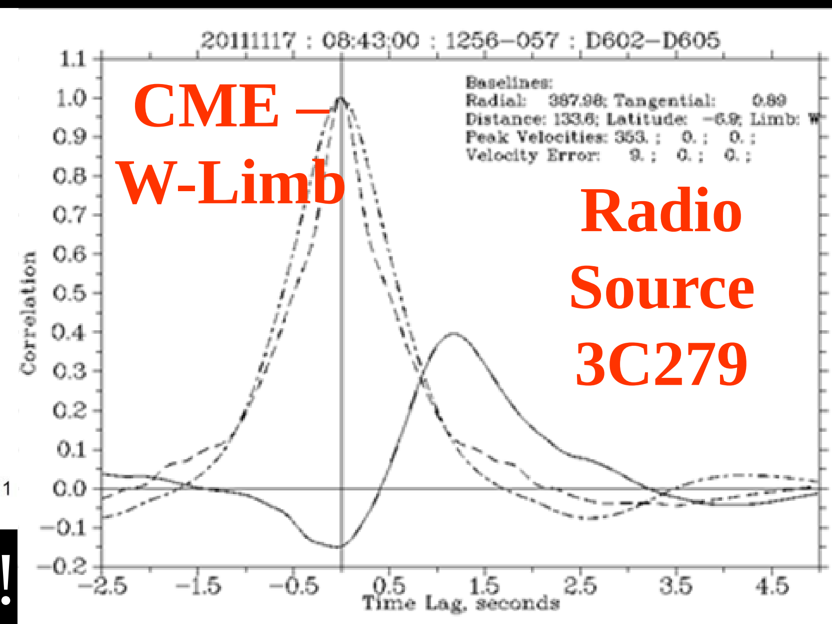

Fully-consistent Results!

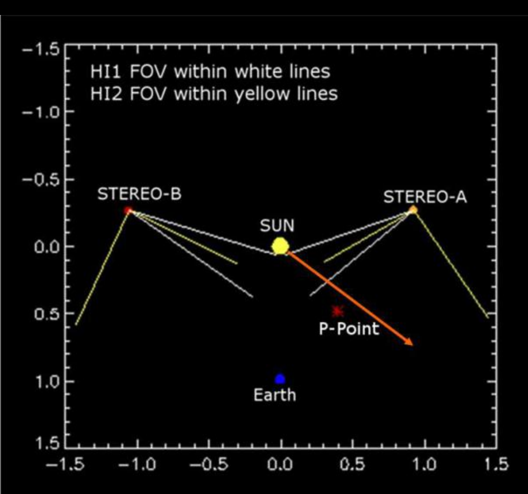

Model Used:	Best Fit in Radial Velocity ($km\,s^{-1}$):	Error in Radial Velocity ($km\,s^{-1}$):
Front:		
Fixed Phi	342.22	12.00
SSEF (30°)	348.83	12.00
Harmonic Mean	352.35	11.00
Middle:		
Fixed Phi	338.36	10.00
SSEF (30°)	343.61	10.00
Harmonic Mean	346.11	9.00
Rear:		
Fixed Phi	335.83	9.00
SSEF (30°)	343.53	8.00
Harmonic Mean	348.37	8.00

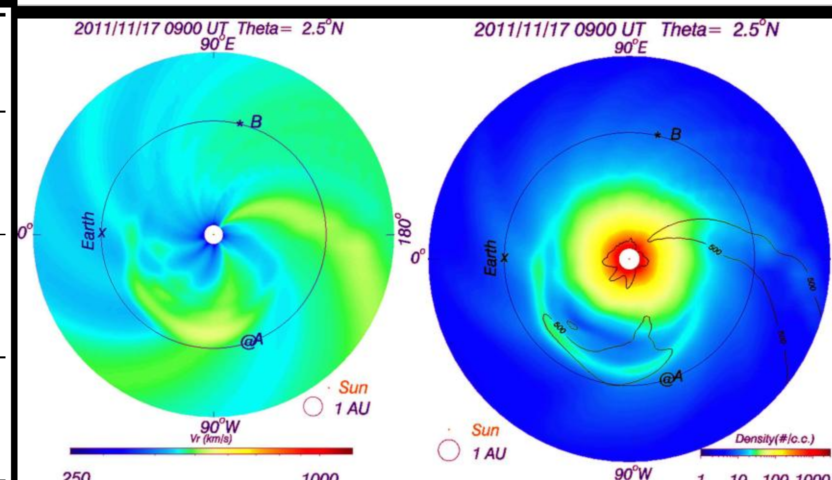

3-D Tomography with Visible-Light Data

2008/04/26-2008/04/30 SOHO|LASCO CME and stream interaction region (SIR) around the declining phase to solar minimum – SMEI data

- Bisi, M.M., B.V. Jackson, A. Buffington, J.M. Clover, P.P. Hick, and M. Tokumaru, "Low-Resolution STELab IPS 3D Reconstructions of the Whole Heliosphere Interval and Comparison with in-Ecliptic Solar Wind Measurements from STEREO and Wind Instrumentation", *Solar Physics "STEREO Science Results at Solar Minimum" Topical Issue*, 256 (1), pp.201-217, doi:10.1007/s11207-009-9350-9, 2009.

Taken from - Jackson, B.V., A. Buffington, P.P. Hick, J.M. Clover, M.M. Bisi, and D.F. Webb, "SMEI 3D Reconstruction of a Coronal Mass Ejection Interacting with a Corotating Solar Wind Density Enhancement: The 2008 April 26 CME", *The Astrophysical Journal*, 724, pp.829–834, doi:10.1088/0004-637X/724/2/829, 2010.

SMEI 3-D Density Reconstruction (1)

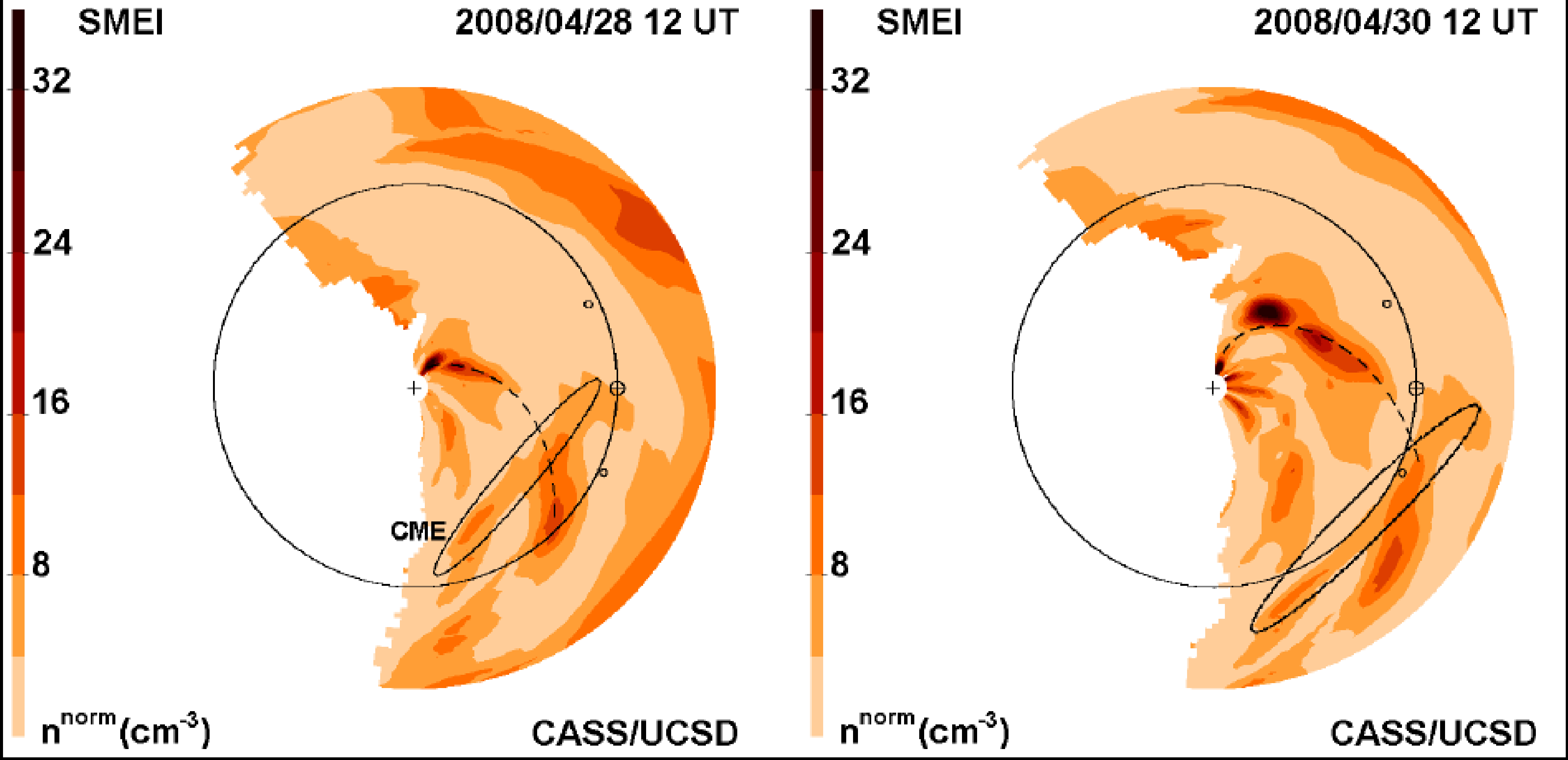

An ecliptic-cut extraction from the UCSD SMEI 3-D reconstruction showing the CME breaking through the CIR as well as the positions of the Sun, Earth, Earth's orbital path, and the two STEREO spacecraft (STEREO-A and STEREO-B).

SMEI 3-D Density Reconstruction (2)

Left-hand difference image shows the various parts of the CME launching off the East limb where two lobe-like features are seen.

Below is an earlier-version ENLIL model with the CME parameterised and input showing CME-CIR interaction.

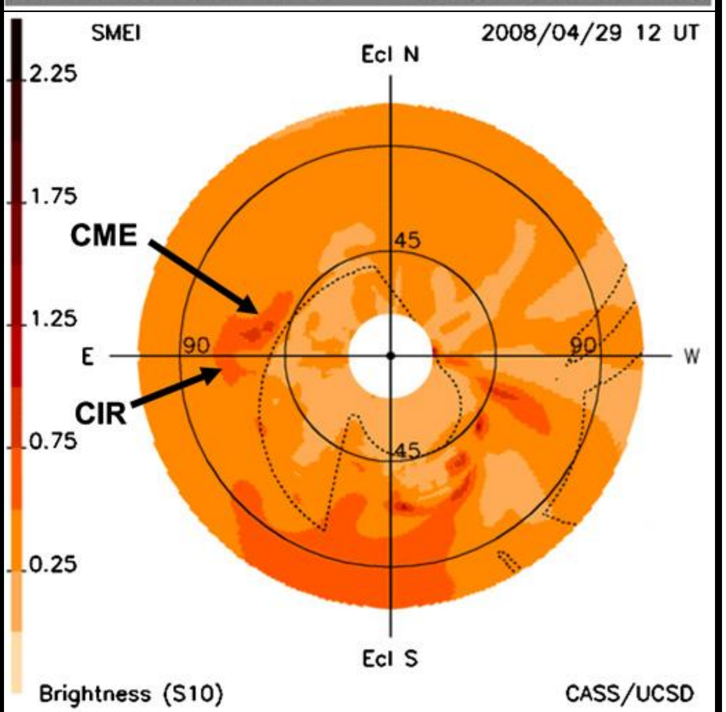

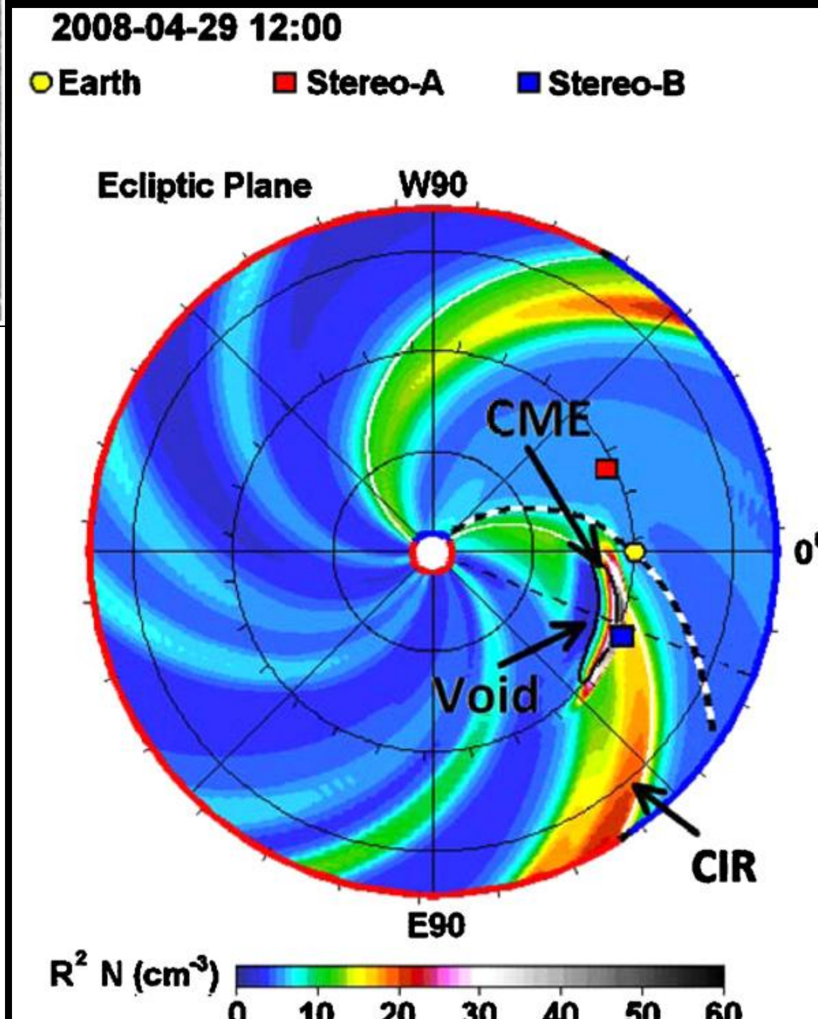

The far-left image is a reconstructed brightness sky image from the SMEI tomography with the exclusion zone around the Sun and the shutter on the innermost camera also outlined – these regions there are no data. Both the CME and CIR are marked off the East limb of the Sun.

SMEI 3-D Density Reconstruction (3)

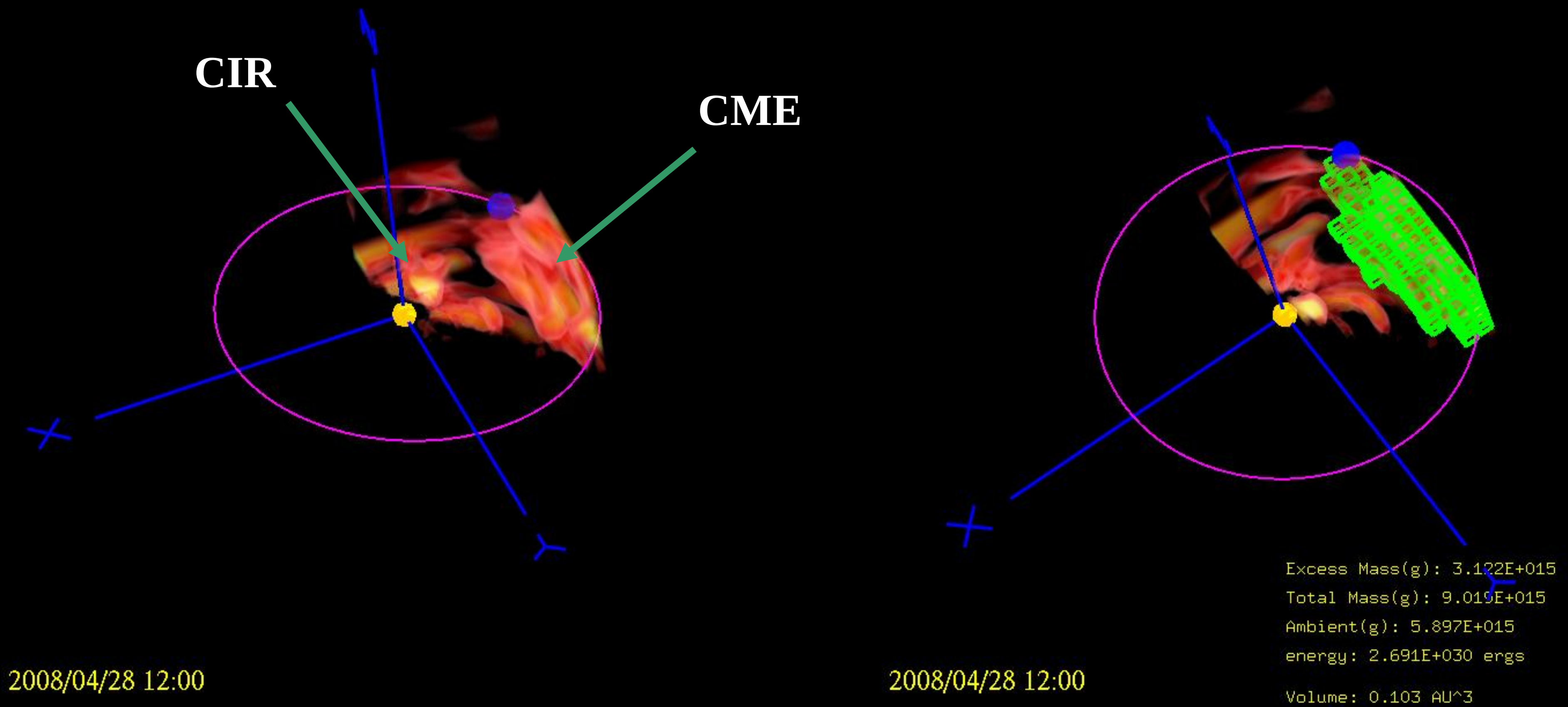

SMEI reconstructed volume (left) and SMEI reconstructed isolated CME portion (right).

Mass of CME from CDAW CME List (LASCO) = 3.4×10^{15} g;
Mass of CME from the SMEI 3D reconstruction = 3.1×10^{15} g.

(Excess mass above the ambient is what is being shown as the CME mass.)

Progress Towards Heliospheric Faraday Rotation (FR) Determination and Verification, Including 3-D Tomography and input to ENLIL MHD Modelling

Combined IPS (60 minutes) and FR (15 minutes) Observations of the Crab Nebula (3C144/PSR B0531+21/PSR J0534+2200) a few Degrees North of the Ecliptic on the Sky Using LOFAR International Stations Plus the Core, Respectively, on 02 July 2014 Commencing at 10:40UT

- Work in progress – publications soon to be in preparation.

Inner-Heliosphere Ecliptic Context (1)

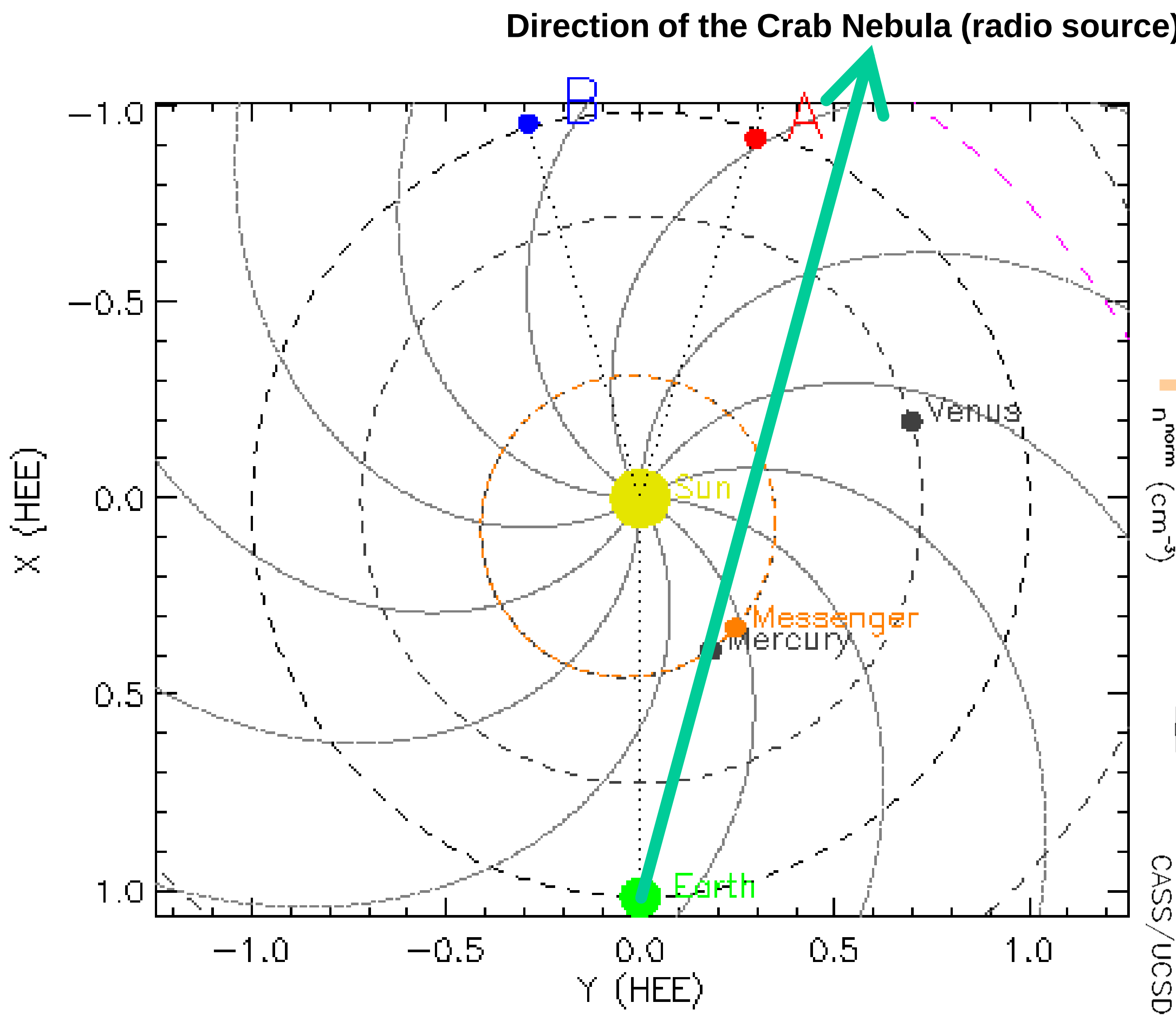

Density at Mercury from the UCSD tomography (using STELab IPS and Wind data) with the $1/R^2$ put back in (since the below image is normalised to 1 AU) provides $n = 31.9\ cm^{-3}$ (low).

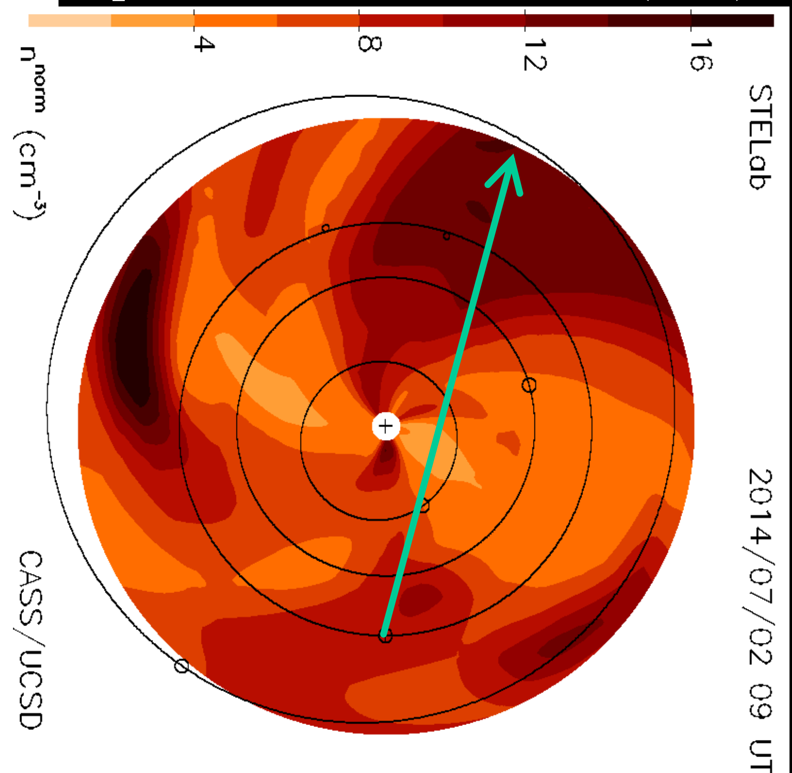

- Left-hand Image courtesy of the STEREO Science Center – Where is STEREO? (http://stereo-ssc.nascom.nasa.gov/cgi-bin/make_where_gif)

Inner-Heliosphere Ecliptic Context (2)

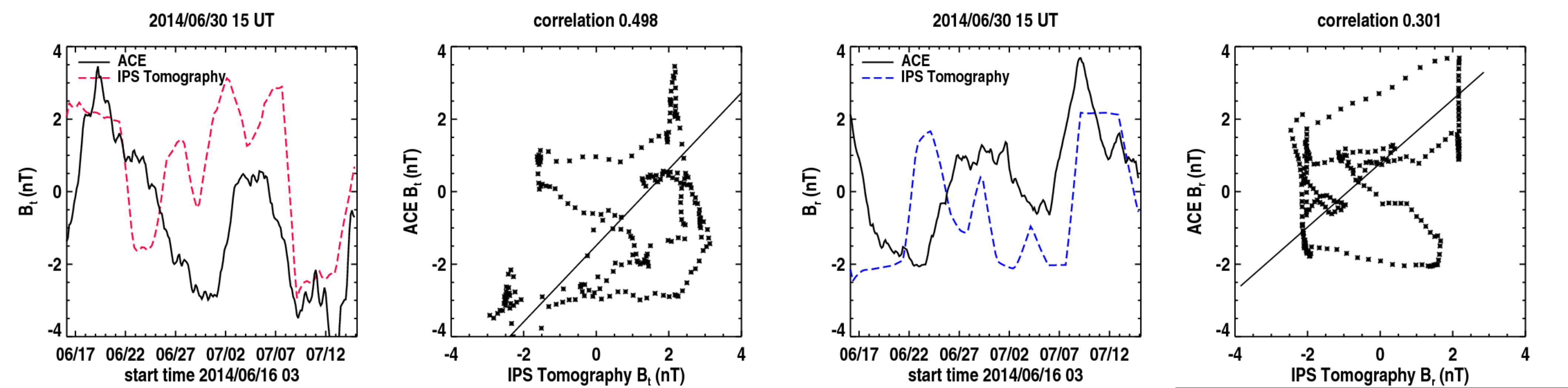

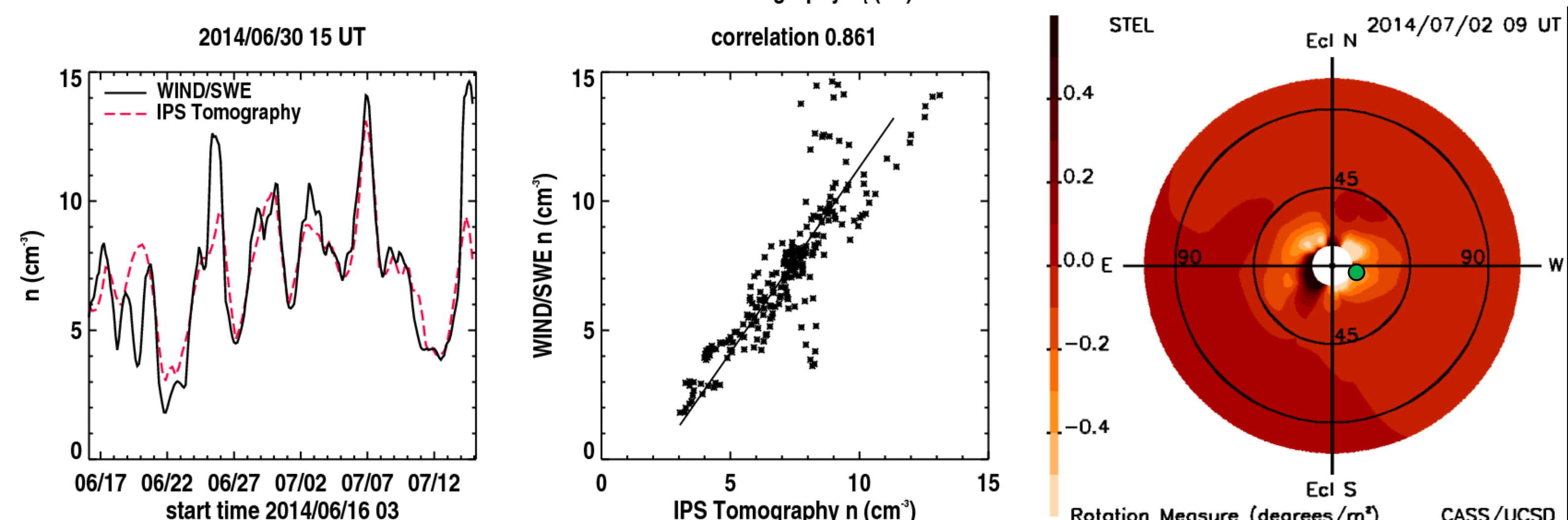

Extractions from the UCSD tomography as labelled incorporating STELab IPS, Wind density and velocity, and NSO Kitt Peak magnetic maps.

- MESSENGER data (courtesy of Dan Gershman, and Jim Raines) for context verification show a velocity ~400 km s^{-1}, but density information is, unfortunately, not available for this period here.

Inner-Heliosphere Ecliptic Context (3)

- ENLIL MHD modelling using the UCSD IPS tomography as input to drive the model (IPS-driven ENLIL) as opposed to using the traditional WSA as input.
- Preliminary results suggest this provides an improved background solar-wind environment in the MHD modelling.

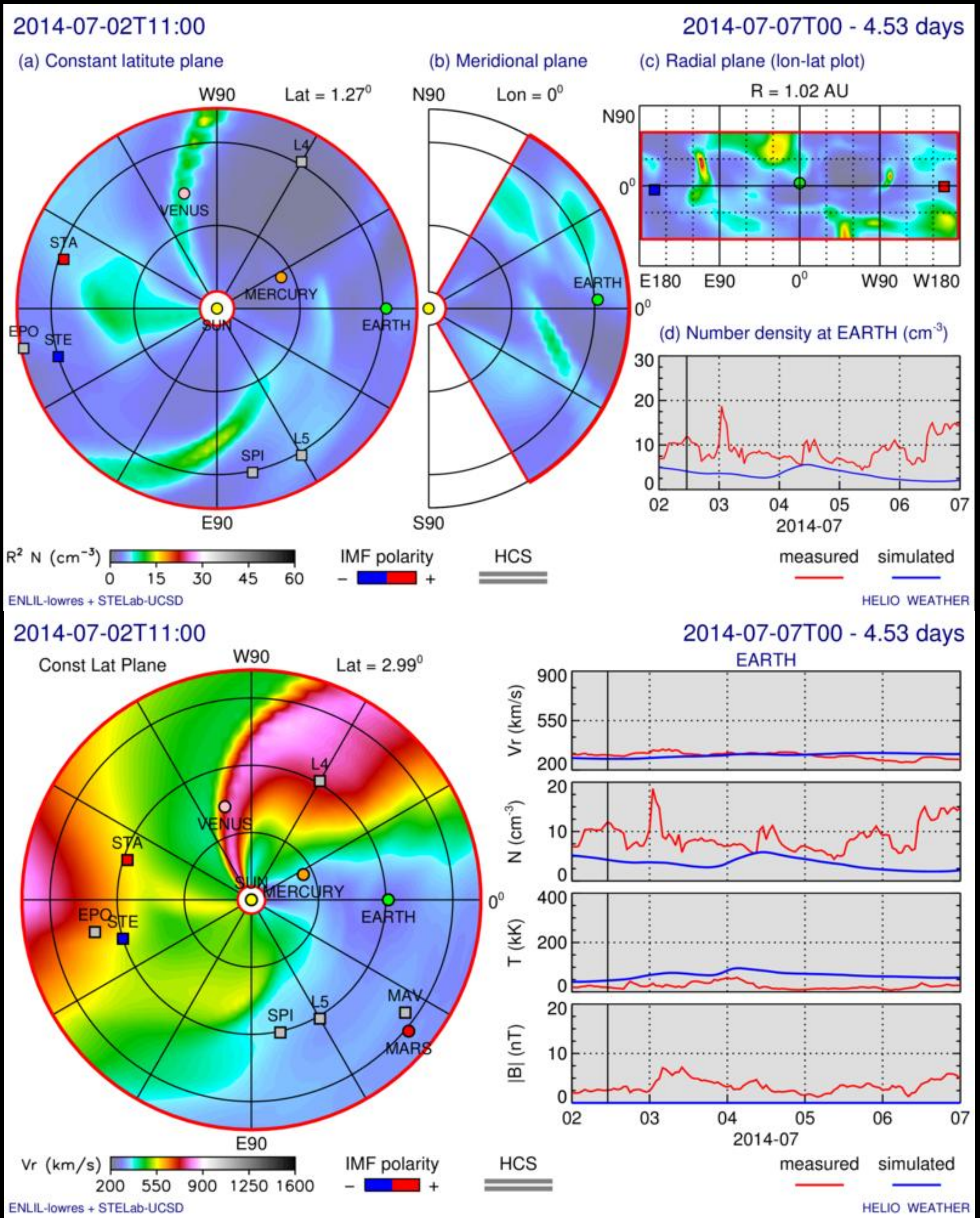

LOFAR Observing Characteristics

- Central observing frequency: 149.609375 MHz ($\lambda \sim 2$ m).
- Observing bandwidth: 78.125 MHz.
- IPS analyses over 15-minute integration times (10:40UT-10:55UT) – only the first 15 minutes used here to match the time of the pulsar observation.

- Pulsar observation analysed by folding the whole data set to obtain the polarised pulse profiles and then these are modelled using an RM fitting routine.
- RM is thus calculated on the integrated 15-minute observation.
- Implications for Space-Weather forecasting at the Earth.

- LOFAR observations of IPS using the international stations yielded a velocity of around 285 km s^{-1}.

Preliminary RM and FR (back-of-envelope calculations)

- The observed RM was: -42.0571 ± 0.02 rad m^{-2}.
- The expected RM of the Crab (at this frequency range) is expected to be: -45.50848 rad m^{-2} (based on anti-solar observations taken during February 2014).
- The modelled ionospheric RM was: 3.11127 ± 0.12935 rad m^{-2}.

- The remaining RM, assumed due to be from the slow solar wind, is: -0.34011 ± 0.15589 rad m^{-2}, *i.e.* **-0.34 ± 0.16 rad m^{-2}** (high?).
- Thus, using FR = λ^2RM (and just using the central frequency), the resulting FR is roughly: -1.36 rad.

- UCSD model RM result is ~ **-0.3° m^{-2}** (factor ~1/57 of LOFAR)?
- Simplification: RM = 0.002 x n_e[cm^{-3}] x B[nT] x L[AU]° m^{-2} where L is the contributing integration length along line of sight = 0.002 x 80 x -150 x 0.4 = **-9.6° m^{-2}** (**-0.168 rad m^{-2}**) (high?).

Next Steps for 3-D Tomography and MHD with Visible-Light Data

HELCATS:

Heliospheric Cataloguing Analysis and Techniques Service

HELCATS is an EU-funded (FP7) initiative to catalogue, model, and validate the resultant kinematic properties of transient (CME) and background (SIR/CIR) solar wind phenomena observed by the UK-led Heliospheric Imager (HI) on NASA's STEREO mission.

WP6: Initialising advances numerical models based on the kinematic properties of STEREO/HI CMEs and CIRs – UPS, Toulouse; GMU, US

(Slide courtesy of Jackie Davies)

Objectives

- To assess the use of HI observations of solar wind streams to initialise numerical models of the background solar wind.
- To assess the use of HI observations of CMEs to inject transients in numerical models of the background solar wind.
- To compare initialisation techniques of MHD codes with HI-assimilated initialisation techniques.
- To establish a catalogue of numerically-predicted CME and shock impacts at in-situ spacecraft and a catalogue of optimised background solar wind and CME simulation results.

http://www.helcats-fp7.eu

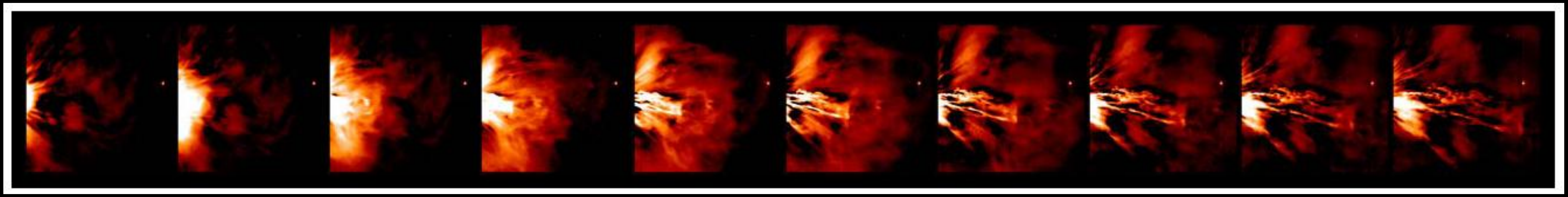

Next Steps for Visible-Light Data and Modelling

- With the ability to propagate out ambient magnetic fields from the Sun, and obtain a reconstruction of B_n at the Earth (see Jackson *et al*., Ap.J.Lett., 803, 2015), if we input higher-resolution visible-light imaging into the tomography from STEREO HIs, for example, this will allow for higher-resolution reconstructions and should provide improved inputs for ENLIL and other MHD modelling. In addition, B_z can now be determined at Earth using the UCSD tomography.

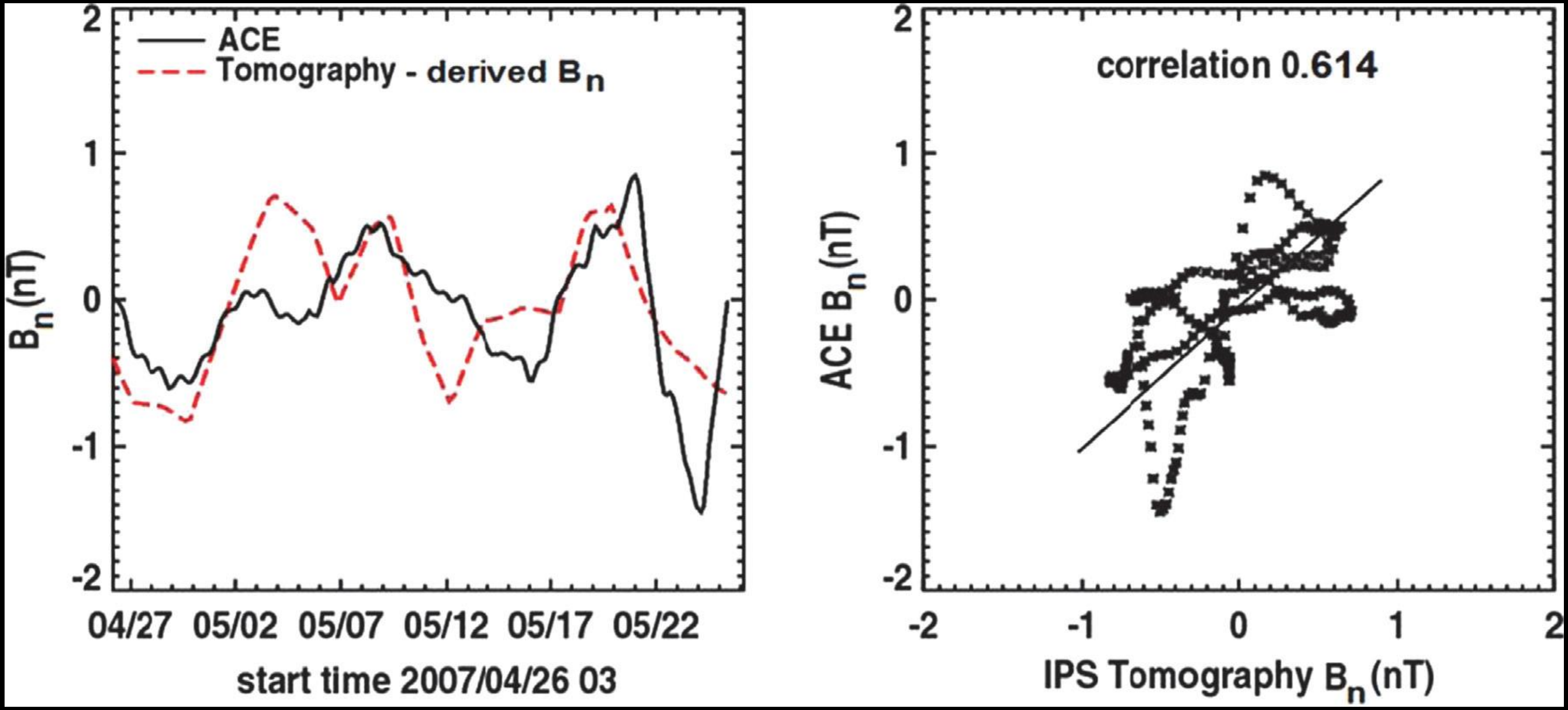

Brief Summary and Outlook to a Long-Standing View from L5

Summary

- Visible-light imaging from L5 will enable long-term enhanced 3-D tomography and MHD modelling from the Sun to the Earth.
- Outlook to constraining ENLIL with visible-light heliospheric imaging (from L5) and potential for data-assimilation techniques.
- IPS combined with visible-light heliospheric imaging is proving to be a powerful combination for scientific studies.
- IPS/FR on LOFAR is progressing very well with good solar wind/ CME results, and preliminary heliospheric RM/FR determination.
- Not discussed here, but could dynamic spectra of near-Sun Type II radio bursts detected with ground-based radio telescopes be used as triggers for burst-mode functionality of L_5-based spacecraft?
- The UCSD 3-D tomography should provide an excellent platform for obtaining 3-D magnetic-field values from combined visible-light and radio observations of FR and IPS (and input to ENLIL).